

PAPER • OPEN ACCESS

Doping dependence of the upper critical field in untwinned $\text{YBa}_2\text{Cu}_3\text{O}_{7-\delta}$ thin films

To cite this article: Eric Wahlberg *et al* 2023 *Supercond. Sci. Technol.* **36** 024001

View the [article online](#) for updates and enhancements.

You may also like

- [Manufacturing and testing of AMaSED-2: a no-insulation high-temperature superconducting demonstrator coil for the space spectrometer ARCOS](#)
Magnus Dam, William Jerome Burger, Rita Carpentiero et al.
- [Thermomagnetic instability and accompanied stress intensity factor jumps in type-II superconducting bulks under various magnetization processes](#)
Chenguang Huang, Zengyu Song, Shaozhen Wang et al.
- [Charge-density-wave tuning in monolayer 1H-TaSe₂ by biaxial strain and charge doping](#)
J. G. Si, M. J. Wei, H. Y. Wu et al.

Doping dependence of the upper critical field in untwinned $\text{YBa}_2\text{Cu}_3\text{O}_{7-\delta}$ thin films

Eric Wahlberg* , Riccardo Arpaia , Alexei Kalaboukhov , Thilo Bauch  and Floriana Lombardi* 

Quantum Device Physics Laboratory, Department of Microtechnology and Nanoscience, Chalmers University of Technology, SE-41296 Göteborg, Sweden

E-mail: ericand@chalmers.se and floriana.lombardi@chalmers.se

Received 6 July 2022, revised 28 October 2022

Accepted for publication 6 December 2022

Published 20 December 2022



Abstract

We report on measurements of the doping dependence of the upper critical field $H_{c,2}$ in 50 nm thick $\text{YBa}_2\text{Cu}_3\text{O}_{7-\delta}$ films. The films are untwinned and are characterized by a small in-plane compressive strain. We find that the $H_{c,2}$ shows a strong decrease in the underdoped region of the phase diagram, in agreement with that which has been measured in relaxed single crystals. The origin of the decrease of $H_{c,2}$ in the underdoped regime is discussed within a scenario where charge density wave (CDW) order competes with superconductivity. This demonstrates the potential of using thin films to study the phase diagram of high- T_c materials under strain, and opens up the possibility for investigating the interplay between CDW order and superconductivity tuned by strain.

Keywords: YBCO thin films, strain, superconductivity

(Some figures may appear in colour only in the online journal)

1. Introduction

The origin of superconductivity in high- T_c cuprates is still an open question, mainly due to the complex intertwining of various electronic orders with the superconductive phenomenon itself. In recent years, the relation between charge density wave (CDW) order and superconductivity has been the subject of intensive investigation [1–5]. It is by now clear that the two orders are competing, which is supported by the strong suppression of T_c at the hole-doping level of $p \approx 0.12$, where CDW order is strongest [2, 6–8]. Another sign of this competition is the rapid decrease of the zero temperature upper critical

field $H_{c,2}(T=0)$ (from now on just $H_{c,2}$) with decreasing doping found in $\text{YBa}_2\text{Cu}_3\text{O}_{7-\delta}$ (YBCO) single crystals [9–13]. According to the thermodynamic Ginzburg–Landau theory, a measure of $H_{c,2} = \Phi_0/2\pi\xi^2$, where Φ_0 is the flux quantum and ξ the superconducting coherence length, allows us to retrieve the doping dependence of the coherence length [9].

Recent experiments have shown that in YBCO $H_{c,2}(p)$ has two maxima: one in the underdoped regime ($p \approx 0.08$) and one in the overdoped regime ($p \approx 0.18$) [12]. These doping levels do not correspond to the maximum superconducting critical temperature T_c , but appear to be connected to the extremes of the doping range where CDW order is present in the phase diagram [3], indicating a strict relation between the two. However, the measurement of $H_{c,2}$ as a function of doping in the cuprates has been controversial [13, 14], with some experiments pointing toward an increase (rather than a decrease) with decreasing doping [15].

To better understand which factors determine the doping dependence of $H_{c,2}$ one can study how it is affected by a tuning

* Authors to whom any correspondence should be addressed.



Original Content from this work may be used under the terms of the [Creative Commons Attribution 4.0 licence](https://creativecommons.org/licenses/by/4.0/). Any further distribution of this work must maintain attribution to the author(s) and the title of the work, journal citation and DOI.

parameter, such as strain. Recent papers have shown that the CDW order can be tuned by strain externally applied to single crystals [4, 16–19]. It has been found that hydrostatic pressure increases T_c and strongly modifies the CDW order [4, 18], while the response to uniaxial strain is more complex [16, 20]. In thin films, the strain can be tuned by the choice of substrate and by varying the film thickness [21, 22], in contrast to the case of single crystals, where complicated apparatus is required to apply the strain, which might not be compatible with high magnetic field facilities and/or other measurement setups.

Here, we show the growth of high-quality thin films of YBCO covering a large part of the phase diagram from $p=0.10$ to $p=0.18$ [23, 24]. We have previously shown that for 50 nm thick slightly overdoped films ($p=0.18$) we can generate a slight compressive uniaxial in-plane strain by using surface reconstructed MgO(110) substrates. MgO(110) is one substrate that allows the growth of untwinned YBCO films [21, 25, 26]. Here, we present structural and electrical transport characterizations of 50 nm thick YBCO films on MgO(110) substrates as a function of doping and show that the underdoped films are untwinned and are strained similarly to the slightly overdoped films. From measurements of the superconducting resistive transition of the films as a function of an applied magnetic field we extract the doping dependence of $H_{c,2}$. The results show that the $H_{c,2}(p)$ behavior in our thin films is in agreement with what has been measured in single crystals [12], with a strong decrease in the underdoped regime. We discuss the origin of this similarity within a scenario where CDW order and superconductivity compete. This work opens up the possibility to study strain dependent superconducting properties, like $H_{c,2}(p)$, by varying the film thickness down to the nanometer scale and/or substrate.

2. Untwinned and underdoped YBCO thin films

The YBCO films used in this experiment are 50 nm thick and are grown by pulsed laser deposition on (110) oriented MgO substrates following a procedure described elsewhere [21, 23]. The films span a wide range of hole-doping p , going from underdoped ($p \approx 0.10$) up to slightly overdoped ($p \approx 0.18$). In this range of p the CDW order grows in strength as the doping is reduced [3], which allows us to study the possible competition between CDW and superconducting orders. The hole-doping of the films is determined by establishing a unique correspondence between p and the out-of-plane lattice parameter c (see [7, 23] for details). To promote the growth of untwinned YBCO films, the substrates are annealed at high temperature ($T=790$ °C) before the film deposition to allow surface reconstruction [21]. The untwinning ratio is estimated from a characterization of the crystal lattice of the YBCO films. Figures 1(a) and (b) show x-ray diffraction (XRD) asymmetric $2\theta-\omega/\omega$ intensity maps around the (308) and (038) YBCO Bragg reflections for a film at $p \approx 0.12$. The two reflections are well separated in 2θ , a consequence of the

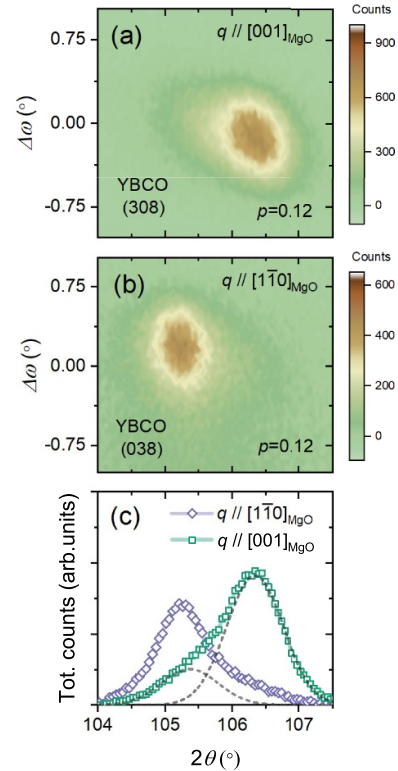


Figure 1. (a) XRD structural characterization of an underdoped YBCO thin film to determine the in-plane structure. (b) $2\theta-\omega/\Delta\omega$ intensity maps around the YBCO (308) and (038) Bragg reflections measured with the scattering vector q directed along the two orthogonal substrate directions MgO $[1\bar{1}0]$ and $[001]$ in an underdoped YBCO thin film ($p=0.12$). (c) Integrated intensity versus 2θ from the maps in (a) and (b). The gray dashed lines show Gaussian fits of the two peaks that build up the total intensity.

orthorhombicity induced by the one-dimensional CuO chains oriented along the YBCO b -axis [27]. We observe that there is a minor (038) component in the (308) map and vice versa, as visualized by the integrated intensity plot in figure 1(c). From the ratio of these two components (see gray dashed lines) we estimate that the films are 83% untwinned. From the 2θ values of the (308) and (038) Bragg reflections and the (00L) Bragg reflections (not shown here) we have extracted the values of the in-plane lattice parameters a and b and the out-of-plane lattice parameter c (see table 1). Compared to YBCO crystals of similar doping [27] the b -axis is slightly shorter and the c -axis slightly longer in the thin films, which is indicative of a uniaxial in-plane compressive strain. The level of in-plane strain ($\delta b = -0.5\%$) is close to what we have previously reported on slightly overdoped YBCO thin films on MgO (see table 1), which means that the strain induced by the substrate does not change much with the doping level of the film. It is well known that strain has an effect on T_c in YBCO [28], which could potentially complicate the determination of the doping level of the films. However, in a previous work [23], where we extracted the phase diagram (T_c versus p) of YBCO thin films grown on MgO and SrTiO₃, which are strained in

Table 1. Comparison of the lattice parameters (in units of Å) of underdoped (slightly overdoped in parenthesis) YBCO thin films and crystals [21, 27].

$p \approx 0.12$ (0.18)	a	b	c
Crystal	3.83 (3.82)	3.89 (3.89)	11.72 (11.69)
Thin film	3.83 (3.82)	3.87 (3.87)	11.73 (11.71)

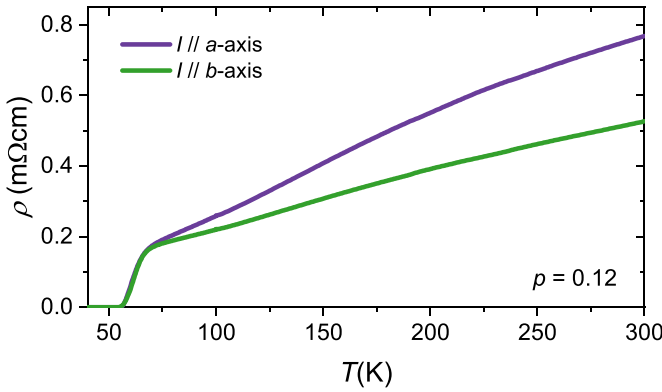


Figure 2. Temperature dependence of the resistivity measured in an untwinned, underdoped YBCO thin film with the current I applied along the YBCO a - and b -axis (purple and green line).

opposite ways (in-plane tensile and compressive respectively), the resulting phase diagram is in good agreement with that of relaxed single crystals [23].

The temperature dependence of the electrical resistance along the YBCO a - and b -axis of an untwinned film measured in a four-point Van der Pauw configuration is shown in figure 2. The resistivity anisotropy (between the YBCO a - and b -axis) is slightly lower than that of completely untwinned crystals at this doping [6], which is consistent with the 83% untwinning ratio of our films. CuO chains along the b -axis in YBCO are the origin of the orthorhombicity of the unit cell. In electrical transport, they cause an in-plane resistivity anisotropy as they are weakly conducting [29, 30].

3. Estimation of $H_{c,2}$

Measurements of the temperature dependence of the electrical resistance $R(T)$ in a range of temperatures around T_c have been performed for 50 nm thick YBCO thin films as a function of doping and magnetic field. Figures 3(a) and (b) show the magnetic field dependence of the resistive transition in a slightly overdoped ($p \approx 0.17$) and an underdoped ($p \approx 0.12$) film. The magnetic field H , spanning the range from 0 to 14 T, is applied perpendicular to the film surface. For each film, we have extracted the magnetic field dependence of the critical temperature $T_c^{0.5R_N}$, which is defined as the temperature at which the resistance has dropped to 50% of the normal state value R_N (see gray dashed line in figures 3(a)–(d)), where R_N is the normal state resistance above the superconducting transition. In conventional superconductors $T_c^{0.5R_N}(H)$ is commonly associated with $H_{c,2}(T)$. This association is

controversial in the high- T_c cuprates since its temperature dependence differs from measurements of $H_{c,2}(T)$ using other methods [31]. However, it has been shown that the $T = 0$ intercept of $T_c(H)$ (regardless of which point of the resistive transition one chooses) can be used to estimate $H_{c,2}(T = 0)$ [14]. Indeed, the $H_{c,2}(T = 0)$ values of YBCO coincide with those extracted by vortex lattice melting fits of $T_c^0(H)$ [12]. A simple estimation of $H_{c,2}(T = 0)$ can be made by making linear fits of $T_c^{0.5R_N}(H)$ (which have been shown to be linear in fields up to at least 60 T [14]) and extrapolate to the $T = 0$ value. Figure 3(c) shows $T_c^{0.5R_N}(H)$ and the linear fits to obtain $H_{c,2}$ for the YBCO thin films with different doping. We observe a clear trend: in films with lower p the magnetic field has a stronger effect on the superconducting transition, indicating a lower $H_{c,2}$ value.

The doping dependence of $H_{c,2}$ extracted in figure 3(c) is presented in figure 4. The values reported come from measurements along the YBCO a -axis, but there is no significant difference in extracting the values from measurements along the b -axis (data not shown here). We find that $H_{c,2}$ drops quickly from ≈ 140 T to ≈ 30 T when the doping is reduced from slightly overdoped to underdoped. This doping trend of $H_{c,2}$ is in excellent agreement with what has been observed in single crystals by various measurement methods (see blue dashed line in figure 4) in the underdoped regime [9, 10, 12, 13, 32]. We therefore conclude that the small in-plane compressive strain induced by the MgO substrate does not have any significant effect on the critical field. The mechanism that causes the drop of $H_{c,2}$ with doping is not completely settled, although it is likely associated with the appearance of CDW order. As mentioned previously, CDW order is present in YBCO in the doping range $p \approx 0.08$ – 0.17 [3]. In the same doping range there is a suppression of T_c compared to the expected approximately parabolic p dependence [6, 7], which is also associated with CDW order [8]. We have previously reported that in similar 30 nm thick YBCO films the suppression of T_c around $p = 0.125$ is reproduced (see pink shaded area in figure 4) [23, 33]. Moreover, we have found by RIXS that CDW order is present in our 50 nm thick films, with characteristics close to those found in single crystals [22]. If the drop of $H_{c,2}$ is a consequence of CDW order, it is therefore not surprising that we find similar values in our thin films as in crystals. It remains to be seen why the uniaxial compressive strain in our film does not produce the same effect on the CDW order as instead happens in single crystals [16].

In the slightly overdoped regime, we find that our data deviate from those reported for single crystals. In the crystal measurements, the maximum $H_{c,2}$ has been estimated to be close to $p \approx 0.18$, though there is a significant uncertainty in this estimation [12]. The exact doping level of the maximum $H_{c,2}$ is crucial to understand the origin of the reduction in the underdoped regime. Some theories of high- T_c superconductivity consider that superconductivity stems from the quantum fluctuations associated with a quantum critical point (QCP) [34]. A QCP close to optimal doping in YBCO has been postulated as the end point of the 3D CDW order, around $p = 0.16$, corresponding to optimal doping [35, 36]. Alternatively, or in addition to that, a putative QCP has been associated to the end

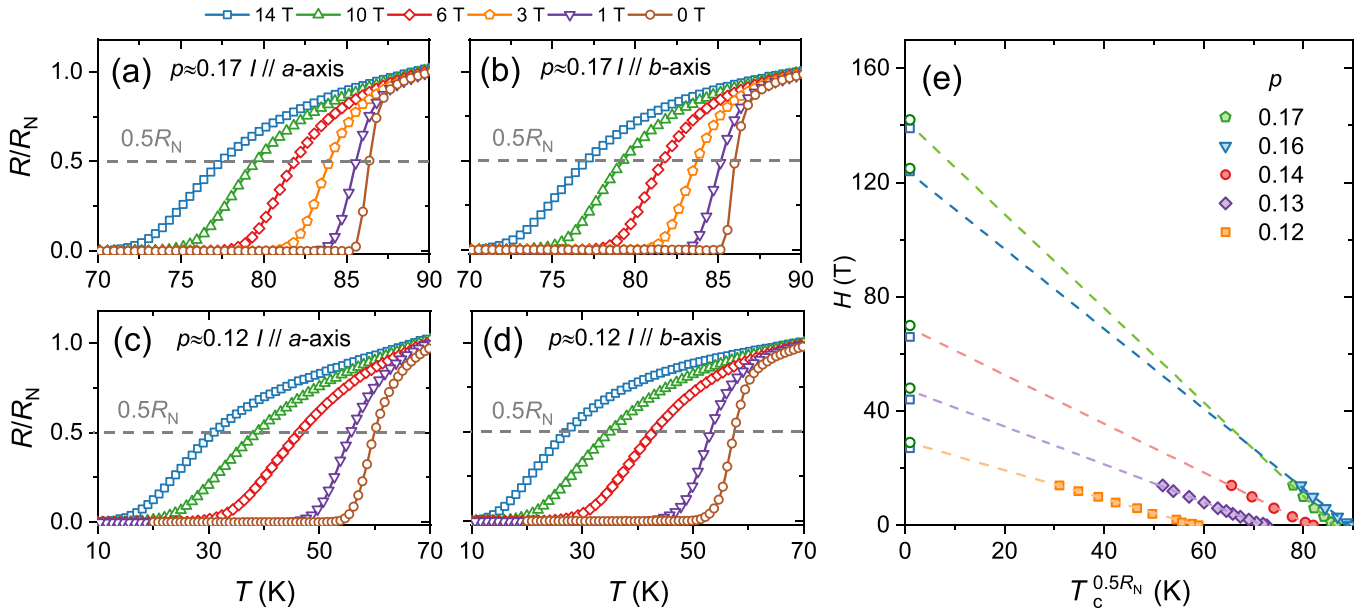


Figure 3. (a)–(d) Magnetic field dependence of the resistive transition in YBCO films at two different doping levels ((a), (b) $p = 0.17$, (c), (d) $p = 0.12$). The magnetic field is applied along the c -axis, perpendicular to the current, which is applied along the a -axis (a), (c), or b -axis (b), (d). The gray dashed lines indicate where the resistance has dropped to 50% of normal state resistance R_N at T_c . (e) Linear fits to $T_c^{0.5R_N}(H)$ for films with different values of p with the current applied along the a -axis. The green open circles show the linear extrapolated values of $H_{c,2}$ at $T_c^{0.5R_N} = 0$. The blue open squares show the linear extrapolated values of $H_{c,2}$ at $T_c^{0.5R_N} = 0$ with the current applied along the b -axis.

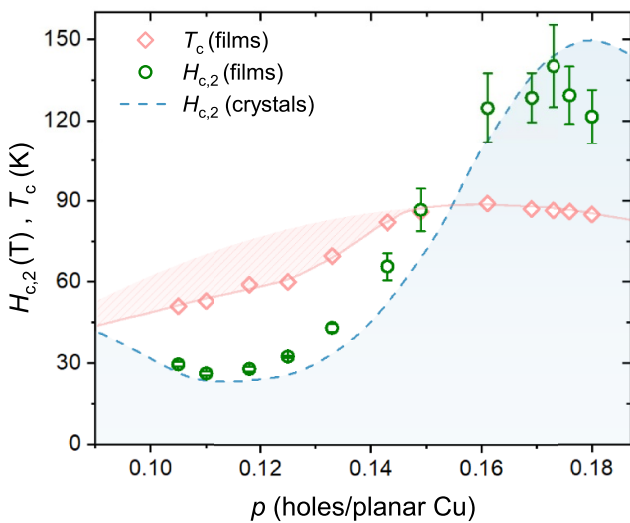


Figure 4. Doping dependence of $H_{c,2}$ (green circles) and T_c (pink squares) for the YBCO thin films. The blue dashed line shows the doping dependence of $H_{c,2}$ measured in YBCO crystals [12]. The pink shaded area shows where T_c is suppressed below the parabolic doping dependence [23].

point of the enigmatic pseudogap phase, at $p \approx 0.19$ [37, 38]. The maximum in $H_{c,2}(p)$ in our measurements is closer to $p \approx 0.17$, which tends to exclude the pseudogap as the origin of the suppression of $H_{c,2}$ at low doping. Nevertheless, the decreased value of $H_{c,2}$ below $p \approx 0.17$ could be related to

the reduced number of states available to superconductivity due to the pseudogap opening and due to the reconstruction of the Fermi surface induced by CDW [39], as some experiments seem to support.

A puzzling observation is that the maximum of $H_{c,2}$ at $p \approx 0.17$ does not correspond to the maximum of T_c , which is at $p = 0.16$ (see figure 4), indicating that the correspondence between the upper critical field and superconductivity is more complex than that which is described by the phenomenological Ginzburg–Landau theory.

4. Conclusions

We present measurements of the upper critical field, $H_{c,2}$ as a function of the doping in 50 nm thick YBCO films. The films are untwinned, with a small in-plane compressive strain along the b -axis. $H_{c,2}(p)$ was estimated by characterizing the magnetic field dependence of the resistive transition. We found that the doping dependence of $H_{c,2}$ measured in single crystals is reproduced in our thin films, with the exception of the doping level above the optimal one ($p > 0.17$). We find no significant difference in the estimated $H_{c,2}(p)$ along the a - and b -axis. These results demonstrate the potential of using thin films to study the phase diagram of high- T_c materials. A major advantage of thin films is that strain can be applied by the substrate in a relatively easy way, which opens up possibilities for future studies of the relation between strain and superconductivity through measurements of $H_{c,2}$ by varying the thickness of the films going to the few nm scale.

Data availability statement

The data that support the findings of this study are available upon reasonable request from the authors.

Acknowledgments

This work was performed in part at Myfab Chalmers, and is supported by the Swedish Research Council (VR) under the Projects 2018-04658 (F L), 2020-04945 (R A) and 2020-05184 (T B).

ORCID iDs

Eric Wahlberg  <https://orcid.org/0000-0002-2723-0688>
 Riccardo Arpaia  <https://orcid.org/0000-0003-4687-2376>
 Alexei Kalaboukhov  <https://orcid.org/0000-0003-2939-6187>
 Thilo Bauch  <https://orcid.org/0000-0002-8918-4293>
 Floriana Lombardi  <https://orcid.org/0000-0002-3478-3766>

References

- [1] Ghiringhelli G *et al* 2012 *Science* **337** 821
- [2] Chang J *et al* 2012 *Nat. Phys.* **8** 871
- [3] Blanco-Canosa S, Frano A, Schierle E, Porras J, Loew T, Minola M, Bluschke M, Weschke E, Keimer B and Tacon M L 2014 *Phys. Rev. B* **90** 054513
- [4] Cyr-Choinière O, LeBoeuf D, Badoux S, Dufour-Beauséjour S, Bonn D, Hardy W, Graf D, Doiron-Leyraud N and Taillefer L 2018 *Phys. Rev. B* **98** 064513
- [5] Arpaia R and Ghiringhelli G 2021 *J. Phys. Soc. Japan* **90** 111005
- [6] Ando Y, Komiya S, Segawa K, Ono S and Kurita Y 2004 *Phys. Rev. Lett.* **93** 267001
- [7] Liang R, Bonn D and Hardy W 2006 *Phys. Rev. B* **73** 180505(R)
- [8] Huecker M *et al* 2014 *Phys. Rev. B* **90** 054514
- [9] Ando Y and Segawa K 2002 *Phys. Rev. Lett.* **88** 167005
- [10] Ramshaw B, Day J, Vignolle B, LeBoeuf D, Dosanjh P, Proust C, Taillefer L, Liang R, Hardy W and Bonn D 2012 *Phys. Rev. B* **86** 174501
- [11] Chang J *et al* 2012 *Nat. Phys.* **8** 751
- [12] Grissonnanche G *et al* 2014 *Nat. Commun.* **5** 1
- [13] Zhou R *et al* 2017 *Proc. Natl Acad. Sci. USA* **114** 13148
- [14] Ando Y *et al* 1999 *Phys. Rev. B* **60** 12475
- [15] Wang Y, Ono S, Onose Y, Gu G, Ando Y, Tokura Y, Uchida S and Ong N 2003 *Science* **299** 86
- [16] Kim H-H *et al* 2018 *Science* **362** 1040
- [17] Kim H-H *et al* 2021 *Phys. Rev. Lett.* **126** 037002
- [18] Souliou S, Gretarsson H, Garbarino G, Bosak A, Porras J, Loew T, Keimer B and Tacon M L 2018 *Phys. Rev. B* **97** 020503(R)
- [19] Choi J *et al* 2022 *Phys. Rev. Lett.* **128** 207002
- [20] Barber M E, Kim H-H, Loew T, Tacon M L, Minola M, Konczykowski M, Keimer B, Mackenzie A and Hicks C W 2021 arXiv:2101.02923 [cond-mat]
- [21] Arpaia R, Andersson E, Kalaboukhov A, Schröder E, Trabaldo E, Ciancio R, Dražić G, Orgiani P, Bauch T and Lombardi F 2019a *Phys. Rev. Mater.* **3** 114804
- [22] Wahlberg E *et al* 2021 *Science* **373** 1506
- [23] Arpaia R, Andersson E, Trabaldo E, Bauch T and Lombardi F 2018 *Phys. Rev. Mater.* **2** 024804
- [24] Baghdadi R, Arpaia R, Bauch T and Lombardi F 2014 *IEEE Trans. Appl. Supercond.* **25** 1
- [25] Dekkers J, Rijnders G, Harkema S, Smilde H, Hilgenkamp H, Rogalla H and Blank D 2003 *Appl. Phys. Lett.* **83** 5199
- [26] Tatsunori O, Hidenori M and Satoshi A 2021 In-plane domain control of rebar coated conductors by annealing under bending strain *IEEE Trans. Appl. Supercond.* **31** 1
- [27] Jorgensen J, Veal B, Paulikas A, Nowicki L, Crabtree G, Claus H and Kwok W 1990 *Phys. Rev. B* **41** 1863
- [28] Welp U, Grimsditch M, Fleshler S, Nessler W, Downey J, Crabtree G and Guimpel J 1992 *Phys. Rev. Lett.* **69** 2130
- [29] Gagnon R, Lupien C and Taillefer L 1994 *Phys. Rev. B* **50** 3458
- [30] Ando Y, Segawa K, Komiya S and Lavrov A 2002 *Phys. Rev. Lett.* **88** 137005
- [31] Welp U, Kwok W, Crabtree G, Vandervoort K and Liu J 1989 *Phys. Rev. Lett.* **62** 1908
- [32] Kačmarčík J *et al* 2018 *Phys. Rev. Lett.* **121** 167002
- [33] Andersson E, Arpaia R, Trabaldo E, Bauch T and Lombardi F 2020 *Supercond. Sci. Technol.* **33** 064002
- [34] Keimer B, Kivelson S, Norman M, Uchida S and Zaanen J 2015 *Nature* **518** 179
- [35] Castellani C, Di Castro C and Grilli M 1996 *Z. Phys. B* **103** 137
- [36] Arpaia R *et al* 2019 *Science* **365** 906
- [37] Ramshaw B *et al* 2015 *Science* **348** 317
- [38] Michon B *et al* 2019 *Nature* **567** 218
- [39] LeBoeuf D *et al* 2007 *Nature* **450** 533